THE JOURNAL OF PHYSICAL CHEMISTRY A
A JOURNAL OF THE AMERICAN CHEMICAL SOCIETY

pubs.acs.org/JPCA Article

Modulating Charge Separation and Intersystem Crossing in Donor–Switch–Acceptor Systems: A Computational Study

Published as part of The Journal of Physical Chemistry virtual special issue "Yoshitaka Tanimura Festschrift".

Yuanyuan Chong, Xiaolong Zhang, Biao Chen, Ran Liu, Ziye Wu, Guoqing Zhang, Jun Jiang, Shaul Mukamel,* and Guozhen Zhang*

Cite This: *J. Phys. Chem. A* 2021, 125, 3088–3094 Read Online

ABSTRACT: Charge separation and intersystem crossing play critical roles in various applications of organic long persistent luminescence materials, including light-emitting diodes, chemical sensors, theranostics, and many biomedical and information applications. Using first-principles calculations, we demonstrate that an azobenzene acting as a photoswitch can be used for altering the configuration of a donor-switch-acceptor (D–S–A) molecular system to ensure charge separation and promote intersystem crossing upon photoexcitation. The trans to cis photoisomerization of an azobenzene switch creates an electron trap that stabilizes the charge-separated state. The cis conformation further facilitates the singlet to triplet intersystem crossing in the excited state. Our theoretical study of the D–S–A system may help the design of long persistent luminescent organic devices.

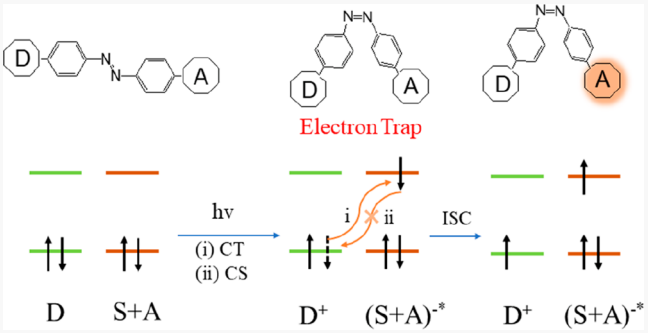

INTRODUCTION

Long persistent luminescence (LPL) has drawn considerable attention owing to its ability to store and slowly release excited-state energy,[1] as well as widespread applications to data encryption,[2,3] solar photovoltaic devices,[4,5] and in vivo biological imaging.[6,7] Inorganic long persistent luminescence materials[8] have emissions that can last for over 10 h.[9] However, their practical applications are often restricted by the high energy consumption in the fabrication and the requirement of expensive noble-metal dopants.[9,10]

Pure organic LPL (OLPL) materials have been recently investigated due to their low cost, easy processability, and design flexibility.[1,6,11] Huang and co-workers have reported a OLPL material with up to 1.35 s lifetime, emitting from a forbidden energy trap state (T_1*) formed by H-aggregation.[12] Its design principle was inspired by the inorganic LPL mechanism, in which a slowly releasing charge carrier trap controls the emission.[1,12] Liu and co-workers have developed a solid-state host–guest complex offering phosphorescence with 2.62 s lifetime, in which the nonradiative relaxation was suppressed by the tight capsulation of guest, thereby achieving a high intersystem crossing (ISC) rate.[13]

Two crucial factors are required to achieve OLPL with afterglow and high phosphorescence quantum yield: a triplet exited state stabilized by an electron trap and a high intersystem crossing rate.[14] The common strategy to create an electron trap is to form a stable charge-separated (CS) excited state.[15,16] This task is challenging because of the fast recominbation of photoexcited charges through the delocalized molecular orbitals in organic molecules. Adachi and others have reported an efficient LPL by ensuring photoinduced CS states via a delicate energy-level engineering of the donor HOMO and the acceptor LUMO.[17−19] Very recently, Tang has reported an excellent OLPL system with up to 7 h afterglow, by an electron trap in a cationic quaternary phosphonium core.[1]

The ISC rate relies on the spin–orbit coupling (SOC) and the singlet–triplet energy gap parameters, according to the empirical formula based on the short-time approximation and first-order perturbation theory:[20−23] $k_{ISC} \propto |\langle S_n|H_{so}|T_m\rangle|^2/(\Delta E_{ST})^2$. Maximizing the SOC matrix element $\langle S_n|H_{so}|T_m\rangle$ and minimizing the energy gap ΔE_{ST} between S_n and T_m states help the ISC process. The SOC parameters for organic chromophores are generally subjected to EI-Sayed's rules, which rely on the transition orbital distributions.[24] While ΔE_{ST} can be decreased by separating geometric centroids between the HOMO and LUMO.[25]

Received: January 6, 2021
Revised: March 13, 2021
Published: April 8, 2021

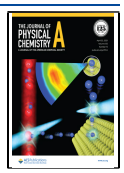

https://doi.org/10.1021/acs.jpca.1c00125
J. Phys. Chem. A 2021, 125, 3088–3094

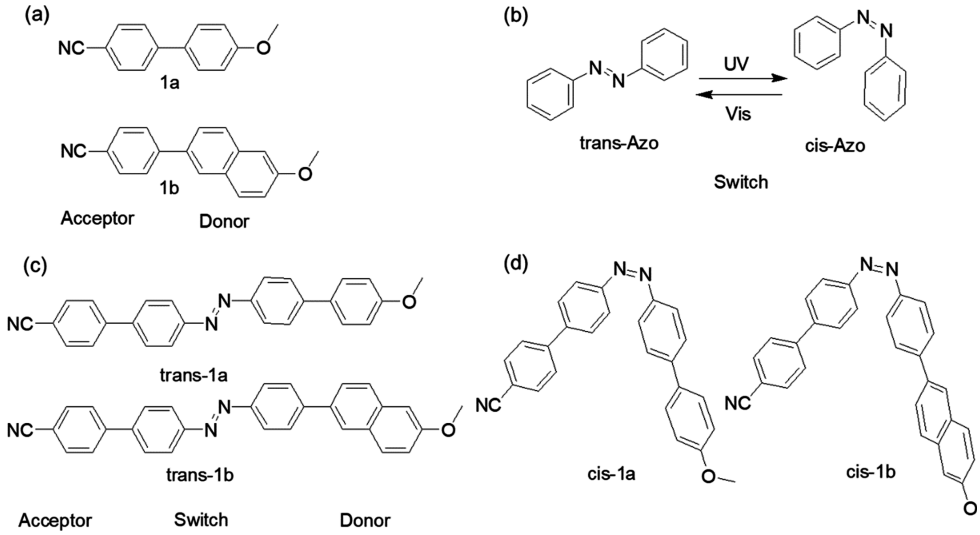

Figure 1. (a) Chemical structures of the donor–acceptor (D–A) molecules **1a** and **1b**. (b) Photoisomerization of the azobenzene (azo) photoswitch. (c) D–S–A molecules *trans*-**1a** and *trans*-**1b** using the trans form of an azo switch to bridge the D–A molecules **1a** and **1b**. (d) Chemical structures of the D–S–A system in the cis form.

Either electron trap formation or ISC rate enhancement have been realized through different strategies, yet they have rarely been jointly incorporated in the same material.

Here we propose a new strategy to achieve this goal by manipulating structures of photoresponsive molecules created by photoinduced conformational isomerization. We have built a donor–switch–acceptor (D–S–A) architecture that inserted an azo photoswitch into a D–A organic fluorescent molecule. The D–S–A adopts the trans form in the ground state, whose S_1 state is a "dark state" and S_2 state is a strong charge transfer (CT) state. Upon excitation to S_2, the electron undergoes intramolecular CT from the donor to the acceptor, accompanied by isomerization from trans (CT channel is "ON") to cis (CT channel is "OFF"). The resulting CS excited state is kept in the cis form, forming a stable electron trap. At the same time, the ISC rate may be promoted because the excited energy levels are shifted by the transformation of the switch bridge. The energy splitting between the first and second excited states S_1 and S_2 ($\Delta E_{S_1S_2}$) is often larger (>1 eV) than that between S_2 and the adjacent triplet state T_m (ΔE_{ST}) (<0.1 eV). The balance between the internal conversion ($S_2 \rightarrow S_1$) and ISC ($S_2 \rightarrow T_m$) may thus shift toward the latter.[26]

■ SIMULATION METHODS

We have designed two D–S–A model systems. When the donor and acceptor in the conventional donor–acceptor (D–A) organic fluorescent molecules are connected with a photoisomerization azobenzene (azo) switch, the D–S–A molecules can take trans → cis conformational transition upon photoexcitation.[27,28] A common cyanophenyl acceptor connects a methoxyphenyl (naphthyl) donor, directly forming parent organic fluorescent D–A molecules **1a** and **1b** adapted from previous experiments,[29] as shown in Figure 1a. It is manifested in Table S1 that **1a** and **1b** have fluorescence luminescence at 352 and 386 nm in tetrahydrofuran, respectively. The azo[30] group (Figure 1b) in its stable trans isomer can be switched to the cis form by ultraviolet (UV) excitation and reversed by visible light (vis) irradiation or heating.[31,32] Using the *trans*-azo to bridge the D–A system, we created two D–S–A molecules in their trans forms (Figure 1c), namely, *trans*-**1a** and -**1b**. Their corresponding cis forms (Figure 1d) are *cis*-**1a** and -**1b**, respectively. The synthesis of these two D–S–A systems is feasible, since the D–A structure in these compounds is similar to azo dyes, which are commonly synthesized by electrophilic aromatic substitution.[33]

First-principles density functional theory (DFT) calculations were carried out using *Gaussian 09*.[34] The ground-state equilibrium structures of both D–A and D–S–A molecules were optimized at the CAM-B3LYP/6-31G(d)[35] level. Time-dependent density functional theory (TDDFT)[36] simulations with the same functional were used for modeling electronic excited states and predicting UV–vis absorption, excited-state energy levels, and photoexcited electron transition. We conducted time-dependent ab initio nonadiabatic molecular dynamic (AI-NAMD) simulation based on surface-hopping method as implemented in Hefei-NAMD,[37] to describe spatial and temporal evolution of the photoexcited electron within the systems. It allows us to qualitatively evaluate the impact of molecular configurations on electron–hole combination. The tetrahydrofuran solvent effect was simulated using the polarizable continuum model (PCM).[38] Computational details are given in Supporting Information.

We found that the D–S–A system in its *trans*-azo form (*trans*-**1a** and -**1b**) is thermodynamically more stable than its cis isomer (*cis*-**1a** and -**1b**),[39] by ∼0.6 eV.

■ RESULTS AND DISCUSSION

Panels a and b of Figure 2 show the computed normalized UV–vis absorption spectra of trans and cis forms of the D–S–A molecules given by Figure 1c,d, respectively. *cis*-**1a** and *cis*-**1b** have the same ∼454 nm absorption peaks, reflecting their similar conjugated backbone. *trans*-**1a** and *trans*-**1b** also exhibit similar absorption bands with peaks at 354 and 358 nm, respectively. Both trans isomers have much stronger ultraviolet absorption than their cis counterparts.

The UV absorption peak at 354 nm (Figure 2a) is ascribed to the second excited state (S_2) of *trans*-**1a** (Figure 2c), which has both characters of CT excitation originated from the HOMO to LUMO transition (78%) and of local excitation rooting from the HOMO−1 to LUMO transition (13%). The

https://doi.org/10.1021/acs.jpca.1c00125
J. Phys. Chem. A 2021, 125, 3088−3094

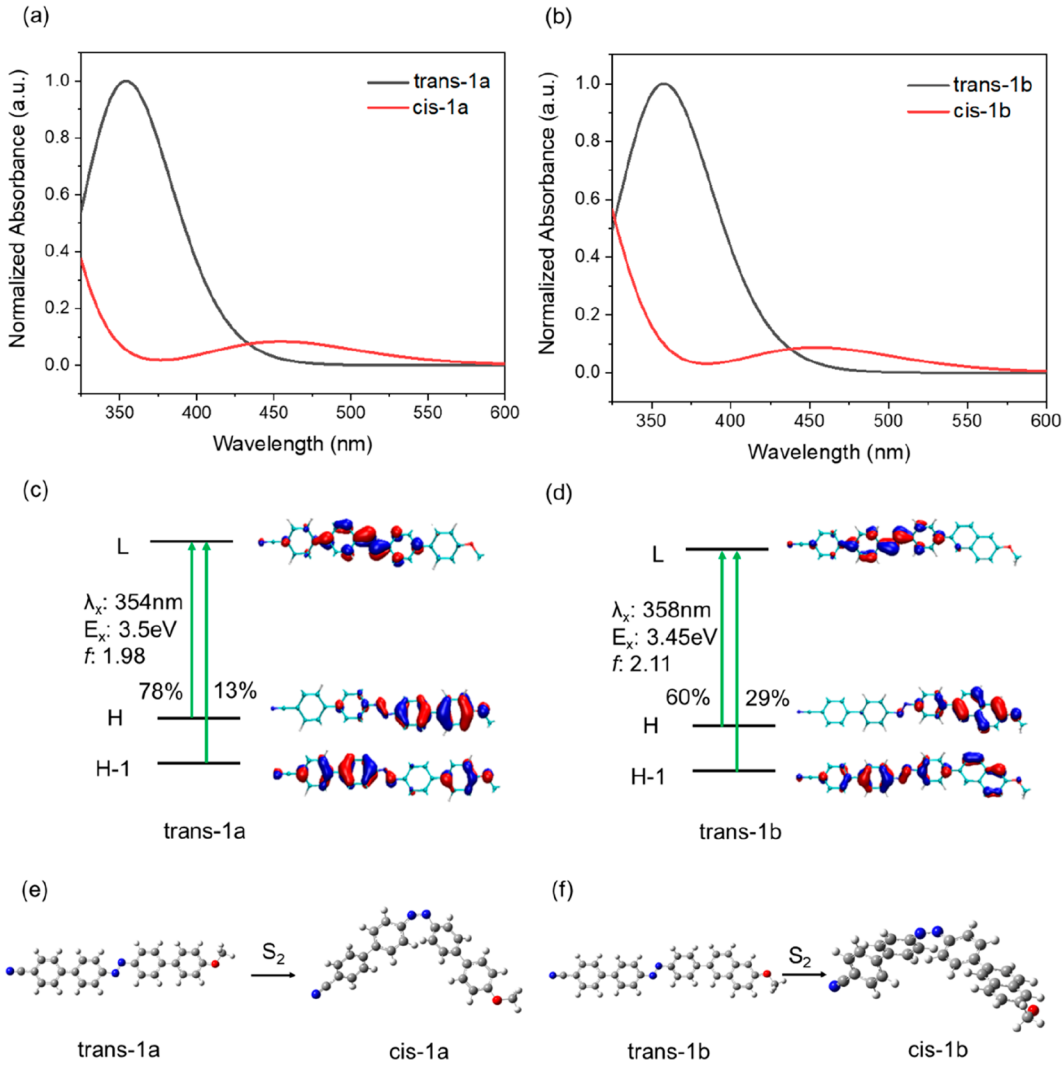

Figure 2. (a, b) Simulated UV−vis absorbance spectra of two D−S−A system molecules. (c, d) Energy scheme presentations of the photoexcitation to the second excited state (S_2) of *trans*-**1a** and *trans*-**1b**, described by the iso-surface of frontier Kohn−Sham orbitals, including H (HOMO), H−1 (HOMO−1), and L (LUMO), absorption wavelength λ_x, excitation energy E_x, and oscillator strength f. (e, f) Geometry optimization of the second excited state (S_2) of *trans*-**1a** and *trans*-**1b** finally leading to their corresponding cis-form *cis*-**1a** and *cis*-**1b** configurations.

absorption maximum of *trans*-**1b** has the same electronic transition features as *trans*-**1a** (Figure 2d). The spatial separation of the HOMO and LUMO (Figure 2c,d) should help electron−hole separation.[25] As the switch is "ON", both transitions show a strong CT character with electrons migrating from the donor to the switch and acceptor moieties. This CT state has stronger excitation as reflected by the doubling of oscillator strength (f = 1.98 in *trans*-**1a** and f = 2.11 in *trans*-**1b**) relative to the original D−A molecules (f = 0.95 in **1a** and f = 0.99 in **1b**, shown in Table S1). At the same time, the first excited states (S_1) of *trans*-**1a** and *trans*-**1b** have virtually no oscillator strength, as shown in Figure S2. S_1 is thus a "dark state" with no fluorescence emission.[40]

Interestingly, the modification of molecular structures usually accompanies the charge transfer excitation, which causes charge redistribution within whole systems.[41] The anionic azo undergoes much more rapid isomerization than its neutral form, because of the lower isomerization energy barrier.[42] Photoexcitation of the *trans*-**1a** and *trans*-**1b** to S_2 will result in electron gain in the azo bridge (Table S3), which is reminiscent of the anionic form azo. No doubt that the concerted inversion pathway after $S_2 \rightarrow S_1$ de-excitation proposed by Diau[43] is dominant in the isomerization of azobenzene. Meanwhile, for the donor−azo−acceptor, chances are that the isomerization could also take place in higher excited states[44,45] owing to the anionic character of the azo moiety after photoexcitation that speeds up isomerization substantially and the competitive time scale of isomerization relative to the internal conversion from S_2 to S_1. We therefore investigated the isomerization of *trans*-**1a** and *trans*-**1b** (Figure 2e,f) in S_2. The resulting cis isomers break the conjugation between donor and acceptor, effectively turning off the CT channel. Electrons trapped in the switch and the acceptor moieties cannot recombine with holes localized on the donor, thus forming the CS state. To verify this electron trapping mechanism, we used the Hefei-NAMD program to simulate the charge dynamics in the cis conformers using a time-dependent surface hopping nonadiabatic molecular dynamics protocol.[37] As can be seen in Figure S4a,b, the electron in the switch and the acceptor does not return to the donor in the cis isomer within 1 ps, indicating that the electron and hole do not recombine in the cis form of D−S−A system; the photoexcited

https://doi.org/10.1021/acs.jpca.1c00125
J. Phys. Chem. A 2021, 125, 3088−3094

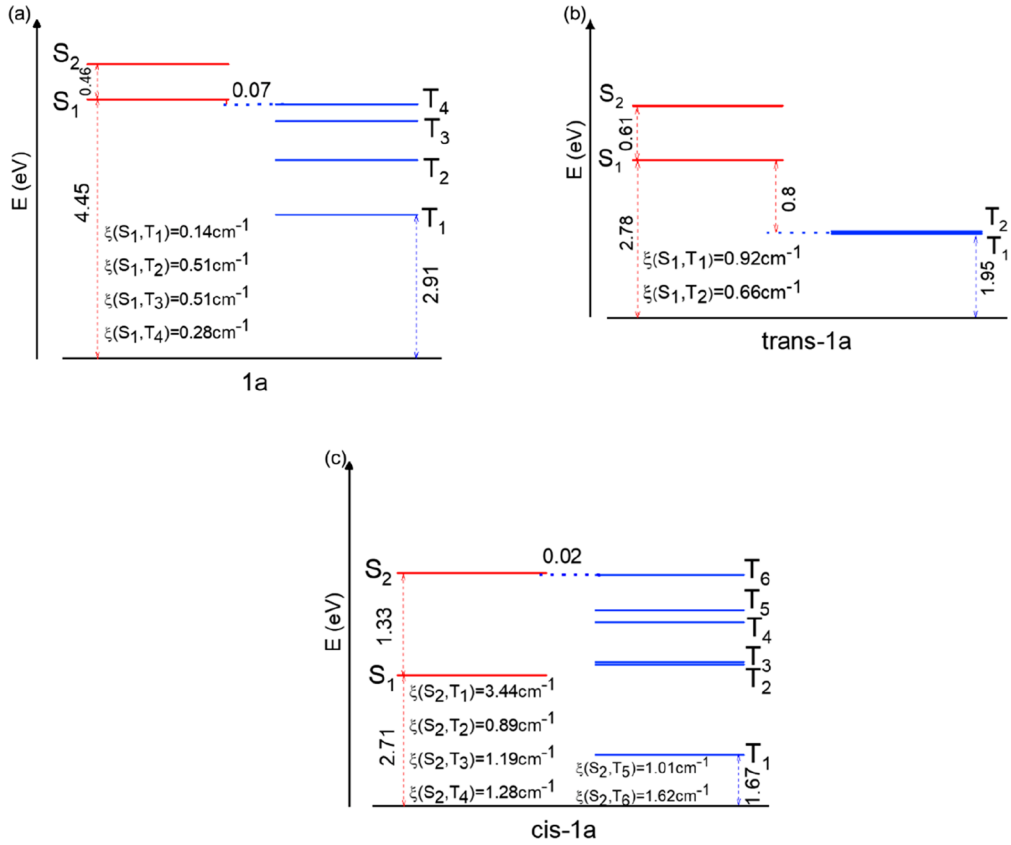

Figure 3. Energy level diagrams of excited states and SOC coefficients (ξ) between different singlet−triplet ISC channels for **1a** (a), *trans*-**1a** (b), and *cis*-**1a** (c). Red lines represent singlet excited-state energy levels, and blue lines represent triplet excited-state energy levels.

CS is well preserved. The NAMD simulations thus support our proposed isomerization-assisted electron trap mechanism in the D−S−A system.

Vertical excitation energies and spin−orbit couplings are two important descriptors of excited-state electronic structure.[46] Among **1a**, *trans*-**1a**, and *cis*-**1a**, *cis*-**1a** has a larger S_2−S_1 energy gap (1.33 eV) than the other two (**1a**, 0.46 eV; *trans*-**1a**, 0.61 eV) (Figure 3). Since a larger S_1−S_2 gap inhibits internal conversion (IC), vibrational relaxation (VR), and fluorescence emission (FE),[26] the *cis*-**1a** is likely to remain on S_2.

As shown in Table 1, the fluorescence rate in *cis*-**1a** (1.60×10^8 s^{-1}) is 4 times smaller than that in **1a** (6.25×10^8 s^{-1}).

Table 1. S_1−S_0 (1a) or S_2−S_0 (*trans*-1a and *cis*-1a) Energy Gap ΔE and Oscillator Strength f at the S_1 Minimum (1a) or S_2 Minimum (*trans*-1a and *cis*-1a) Structures and the Fluorescence Rate (k_{FL}) and Fluorescence Lifetime (τ_{FL}) of Molecules 1a, *trans*-1a, and *cis*-1a

	ΔE (eV)	f	k_{FL} (10^8 s^{-1})	τ_{FL} (ns)
1a (S_1)	−3.75	1.01	6.25	1.60
trans-**1a** (S_2)	−2.92	1.98	7.37	1.36
cis-**1a** (S_2)	−2.80	0.47	1.60	6.25

This reduction is attributed to the smaller S_n−S_0 gap and the corresponding oscillator strength. Ma et al. proposed that the phosphorescence can be effectively restrained if the T_2−T_1 energy gap ($\Delta E_{T_1T_2}$) is much larger than the T_2−S_n energy gap (ΔE_{ST}),[26] which is similar to that for *cis*-**1a**, as seen in Figure 3c. We therefore expect that the fluorescence of *cis*-**1a** will be substantially inhibited.

The ISC rate of *cis*-**1a** increases 26-fold relative to **1a** (Table 2), which is the result of joining contributions from the increase of SOC coefficient of the specific ISC channel (*cis*-**1a**, 1.62 cm^{-1} for S_2−T_6; **1a**, 0.28 cm^{-1} for S_1−T_4) and the decrease of corresponding singlet−triplet energy gap (*cis*-**1a**, 0.02 eV; **1a**, 0.07 eV).

To verify that the electron trap formed in the singlet state retains its triplet character, we conducted natural transition orbital (NTO)[47] analysis for the T_1 state in cis forms. The dominant NTOs indicate that electrons transferred from the donor will be located at the switch and acceptor in T_1 (Figure S5).

Likewise, the photophysical properties of 1b and its azo derivatives (*trans*-**1b** and *cis*-**1b**) are similar to their counterparts of **1a**, indicating that **1b** fits the D−S−A model as well. More detail is given in Supporting Information (Figure S6, Table S4, Table S5).

■ CONCLUSIONS

We have presented a practical strategy for creating a stable electron trap and enhancing the ISC rates in organic complexes. We have examined a model D−S−A system, created by inserting an azo photoswitch into a D−A type organic fluorescent molecule. The D−S−A favors the trans form in its ground state, where the S_1 state is dark and S_2 has a strong CT character from the donor to the switch and the acceptor with strong absorption. Upon photoexcitation to S_2, this system undergoes intramolecular CT, accompanied by trans (charge transport channel is "ON") to cis (charge transport channel is "OFF") isomerization. The resulting CS excited state is then kept in the cis form. At the same time, the

https://doi.org/10.1021/acs.jpca.1c00125
J. Phys. Chem. A 2021, 125, 3088−3094

Table 2. S_n−T_m Energy Gap (ΔE_{ST}), Reorganization Energy (λ), and SOC Coefficients (V_{SOC}) at the S_0 Minimum Structures and the ISC Rate (k_{ISC}), ISC Rate Relative to D−A Molecule 1a (k_{rel}) and ISC Lifetime (τ_{ISC}) of Molecules 1a, *trans*-1a, and *cis*-1a

		ΔE_{ST} (eV)	λ (eV)	V_{SOC} (cm^{-1})	k_{ISC} (s^{-1})	k_{rel}	τ_{ISC} (s)
1a	S_1−T_4	−0.07	−0.21	0.28	3.65×10^7	1	2.74×10^{-8}
trans-**1a**	S_1−T_2	−0.80	−0.72	0.66	2.42×10^4	6.63×10^{-4}	4.14×10^{-5}
cis-**1a**	S_1−T_1	−1.05	−1.51	0.20	7.68×10^3	2.10×10^{-4}	1.30×10^{-4}
	S_2−T_6	−0.02	−0.49	1.62	9.57×10^8	26.22	1.05×10^{-9}

shifting of energy levels of the excited state due to structural changes leads to large energy splitting between S_2 and S_1 ($\Delta E_{S_1S_2}$) as well as a small energy gap between S_2 and T_m (ΔE_{ST}) in cis-form molecules. These changes effectively promote the ISC of photoexcited D−S−A while restraining its fluorescent emission. Our theoretical results suggest a novel strategy for combining stable electron trap and promoting intersystem crossing toward molecular design of OLPL, which may be applied in the fields of afterglow, biological sensors, and optical recording devices.

■ ASSOCIATED CONTENT

Supporting Information

The Supporting Information is available free of charge at https://pubs.acs.org/doi/10.1021/acs.jpca.1c00125.

> Computational method, absorption and emission properties of the D−A system, electron transition of D−S−A molecules, PES scanning (including NBO charge profiles), ultrafast electron evolution process (including spatial electron distribution graphs), NTO analysis, the extendibility of the D−S−A model (including energy level diagrams and tables of energy gaps and oscillator strengths) (PDF)

■ AUTHOR INFORMATION

Corresponding Authors

Shaul Mukamel − *Department of Chemistry and Department of Physics & Astronomy, University of California, Irvine, California 92697, United States;* orcid.org/0000-0002-6015-3135; Email: smukamel@uci.edu

Guozhen Zhang − *Hefei National Laboratory for Physical Sciences at the Microscale, CAS Center for Excellence in Nanoscience, School of Chemistry and Materials Science, University of Science and Technology of China, Hefei, Anhui 230026, P. R. China;* orcid.org/0000-0003-0125-9666; Email: guozhen@ustc.edu.cn

Authors

Yuanyuan Chong − *Hefei National Laboratory for Physical Sciences at the Microscale, CAS Center for Excellence in Nanoscience, School of Chemistry and Materials Science, University of Science and Technology of China, Hefei, Anhui 230026, P. R. China*

Xiaolong Zhang − *Hefei National Laboratory for Physical Sciences at the Microscale, CAS Center for Excellence in Nanoscience, School of Chemistry and Materials Science, University of Science and Technology of China, Hefei, Anhui 230026, P. R. China*

Biao Chen − *Hefei National Laboratory for Physical Sciences at the Microscale, CAS Center for Excellence in Nanoscience, School of Chemistry and Materials Science, University of Science and Technology of China, Hefei, Anhui 230026, P. R. China*

Ran Liu − *Hefei National Laboratory for Physical Sciences at the Microscale, CAS Center for Excellence in Nanoscience, School of Chemistry and Materials Science, University of Science and Technology of China, Hefei, Anhui 230026, P. R. China; MOE Key Laboratory of Organic OptoElectronics and Molecular Engineering, Department of Chemistry, Tsinghua University, Beijing 100084, P. R. China*

Ziye Wu − *Hefei National Laboratory for Physical Sciences at the Microscale, CAS Center for Excellence in Nanoscience, School of Chemistry and Materials Science, University of Science and Technology of China, Hefei, Anhui 230026, P. R. China; School of Information, Guizhou University of Finance and Economics, Guiyang 550025, P. R. China*

Guoqing Zhang − *Hefei National Laboratory for Physical Sciences at the Microscale, CAS Center for Excellence in Nanoscience, School of Chemistry and Materials Science, University of Science and Technology of China, Hefei, Anhui 230026, P. R. China;* orcid.org/0000-0003-3155-8915

Jun Jiang − *Hefei National Laboratory for Physical Sciences at the Microscale, CAS Center for Excellence in Nanoscience, School of Chemistry and Materials Science, University of Science and Technology of China, Hefei, Anhui 230026, P. R. China;* orcid.org/0000-0002-6116-5605

Complete contact information is available at: https://pubs.acs.org/10.1021/acs.jpca.1c00125

Notes

The authors declare no competing financial interest.

■ ACKNOWLEDGMENTS

This work was financially supported by the National Key Research and Development Program of China (2018YFA0208603), the National Natural Science Foundation of China (21633006, 21703221), DNL Cooperation Fund CAS (No. DNL201913). S.M. is grateful for the support of NSF grant CHE-1953045. The Supercomputing Center of University of Science and Technology of China is acknowledged for providing computing resource.

■ REFERENCES

(1) Alam, P.; Leung, N. L.; Liu, J.; Cheung, T. S.; Zhang, X.; He, Z.; Kwok, R. T.; Lam, J. W.; Sung, H. H.; Williams, I. D.; et al. Two Are Better Than One: A Design Principle for Ultralong-Persistent Luminescence of Pure Organics. *Adv. Mater.* **2020**, *32* (22), 2001026.

(2) Cai, S.; Shi, H.; Li, J.; Gu, L.; Ni, Y.; Cheng, Z.; Wang, S.; Xiong, W. w.; Li, L.; An, Z. Visible-Light-Excited Ultralong Organic Phosphorescence by Manipulating Intermolecular Interactions. *Adv. Mater.* **2017**, *29* (35), 1701244.

(3) Xu, S.; Chen, R.; Zheng, C.; Huang, W. Excited State Modulation for Organic Afterglow: Materials and Applications. *Adv. Mater.* **2016**, *28* (45), 9920−9940.

(4) Liang, Y.-J.; Liu, F.; Chen, Y.-F.; Wang, X.-J.; Sun, K.-N.; Pan, Z. New Function of the Yb^{3+} Ion as an Efficient Emitter of Persistent Luminescence in the Short-Wave Infrared. *Light: Sci. Appl.* **2016**, *5* (7), No. e16124.
(5) Yang, X.; Zhou, G.; Wong, W.-Y. Functionalization of Phosphorescent Emitters and Their Host Materials by Main-Group Elements for Phosphorescent Organic Light-Emitting Devices. *Chem. Soc. Rev.* **2015**, *44* (23), 8484−8575.
(6) Tan, H.; Wang, T.; Shao, Y.; Yu, C.; Hu, L. Crucial Breakthrough of Functional Persistent Luminescence Materials for Biomedical and Information Technological Applications. *Front. Chem.* **2019**, *7* (387), 31214570.
(7) Palner, M.; Pu, K.; Shao, S.; Rao, J. Semiconducting Polymer Nanoparticles with Persistent near-Infrared Luminescence for in Vivo Optical Imaging. *Angew. Chem., Int. Ed.* **2015**, *54* (39), 11477−11480.
(8) Van den Eeckhout, K.; Smet, P. F.; Poelman, D. Persistent Luminescence in Eu^{2+}-Doped Compounds: A Review. *Materials* **2010**, *3* (4), 2536−2566.
(9) Matsuzawa, T.; Aoki, Y.; Takeuchi, N.; Murayama, Y. A New Long Phosphorescent Phosphor with High Brightness, $SrAl_2O_4$: Eu^{2+}, Dy^{3+}. *J. Electrochem. Soc.* **1996**, *143* (8), 2670−2673.
(10) Yamamoto, H.; Matsuzawa, T. Mechanism of Long Phosphorescence of $SrAl_2O_4$: Eu^{2+}, Dy^{3+} and $CaAl_2O_4$: Eu^{2+}, Nd^{3+}. *J. Lumin.* **1997**, *72*, 287−289.
(11) Im, Y.; Kim, M.; Cho, Y. J.; Seo, J.-A.; Yook, K. S.; Lee, J. Y. Molecular Design Strategy of Organic Thermally Activated Delayed Fluorescence Emitters. *Chem. Mater.* **2017**, *29* (5), 1946−1963.
(12) An, Z.; Zheng, C.; Tao, Y.; Chen, R.; Shi, H.; Chen, T.; Wang, Z.; Li, H.; Deng, R.; Liu, X.; et al. Stabilizing Triplet Excited States for Ultralong Organic Phosphorescence. *Nat. Mater.* **2015**, *14* (7), 685−90.
(13) Zhang, Z.-Y.; Liu, Y. Ultralong Room-Temperature Phosphorescence of a Solid-State Supramolecule between Phenylmethylpyridinium and Cucurbit[6]Uril. *Chem. Sci.* **2019**, *10* (33), 7773−7778.
(14) Kenry; Chen, C.; Liu, B. Enhancing the Performance of Pure Organic Room-Temperature Phosphorescent Luminophores. *Nat. Commun.* **2019**, *10* (1), 2111.
(15) Leytner, S.; Hupp, J. T. Evaluation of the Energetics of Electron Trap States at the Nanocrystalline Titanium Dioxide/Aqueous Solution Interface Via Time-Resolved Photoacoustic Spectroscopy. *Chem. Phys. Lett.* **2000**, *330* (3−4), 231−236.
(16) Wu, K.; Zhu, H.; Liu, Z.; Rodríguez-Córdoba, W.; Lian, T. Ultrafast Charge Separation and Long-Lived Charge Separated State in Photocatalytic Cds−Pt Nanorod Heterostructures. *J. Am. Chem. Soc.* **2012**, *134* (25), 10337−10340.
(17) Ohkita, H.; Sakai, W.; Tsuchida, A.; Yamamoto, M. Charge Recombination Luminescence Via the Photoionization of a Dopant Chromophore in Polymer Solids. *Macromolecules* **1997**, *30* (18), 5376−5383.
(18) Lewis, G. N.; Lipkin, D. Reversible Photochemical Processes in Rigid Media: The Dissociation of Organic Molecules into Radicals and Ions. *J. Am. Chem. Soc.* **1942**, *64* (12), 2801−2808.
(19) Kabe, R.; Adachi, C. Organic Long Persistent Luminescence. *Nature* **2017**, *550* (7676), 384−387.
(20) Chen, Y. L.; Li, S. W.; Chi, Y.; Cheng, Y. M.; Pu, S. C.; Yeh, Y. S.; Chou, P. T. Switching Luminescent Properties in Osmium-Based B-Diketonate Complexes. *ChemPhysChem* **2005**, *6* (10), 2012−2017.
(21) Shuai, Z.; Peng, Q. Organic Light-Emitting Diodes: Theoretical Understanding of Highly Efficient Materials and Development of Computational Methodology. *NATL SCI REV* **2017**, *4* (2), 224−239.
(22) Shuai, Z.; Peng, Q. Excited States Structure and Processes: Understanding Organic Light-Emitting Diodes at the Molecular Level. *Phys. Rep.* **2014**, *537* (4), 123−156.
(23) Obara, S.; Itabashi, M.; Okuda, F.; Tamaki, S.; Tanabe, Y.; Ishii, Y.; Nozaki, K.; Haga, M.-a. Highly Phosphorescent Iridium Complexes Containing Both Tridentate Bis (Benzimidazolyl)-Benzene or-Pyridine and Bidentate Phenylpyridine: Synthesis, Photophysical Properties, and Theoretical Study of Ir-Bis (Benzimidazolyl) Benzene Complex. *Inorg. Chem.* **2006**, *45* (22), 8907−8921.
(24) El-Sayed, M. A. Spin—Orbit Coupling and the Radiationless Processes in Nitrogen Heterocyclics. *J. Chem. Phys.* **1963**, *38* (12), 2834−2838.
(25) Zhou, M.; Higaki, T.; Hu, G.; Sfeir, M. Y.; Chen, Y.; Jiang, D.-e.; Jin, R. Three-Orders-of-Magnitude Variation of Carrier Lifetimes with Crystal Phase of Gold Nanoclusters. *Science* **2019**, *364* (6437), 279−282.
(26) Xu, Y.; Liang, X.; Zhou, X.; Yuan, P.; Zhou, J.; Wang, C.; Li, B.; Hu, D.; Qiao, X.; Jiang, X.; et al. Highly Efficient Blue Fluorescent Oleds Based on Upper Level Triplet-Singlet Intersystem Crossing. *Adv. Mater.* **2019**, *31* (12), No. e1807388.
(27) Satzger, H.; Root, C.; Braun, M. Excited-State Dynamics of Trans-and Cis-Azobenzene after Uv Excitation in the $\pi\pi^*$ Band. *J. Phys. Chem. A* **2004**, *108* (30), 6265−6271.
(28) Wu, Z.; Cui, P.; Zhang, G.; Luo, Y.; Jiang, J. Self-Adaptive Switch Enabling Complete Charge Separation in Molecular-Based Optoelectronic Conversion. *J. Phys. Chem. Lett.* **2018**, *9* (4), 837−843.
(29) Chen, B.; Zhang, X.; Wang, Y.; Miao, H.; Zhang, G. Aggregation-Induced Emission with Long-Lived Room-Temperature Phosphorescence from Methylene-Linked Organic Donor−Acceptor Structures. *Chem. - Asian J.* **2019**, *14* (6), 751−754.
(30) Weis, P.; Wu, S. Light-Switchable Azobenzene-Containing Macromolecules: From Uv to near Infrared. *Macromol. Rapid Commun.* **2018**, *39* (1), 1700220.
(31) Bandara, H. D.; Burdette, S. C. Photoisomerization in Different Classes of Azobenzene. *Chem. Soc. Rev.* **2012**, *41* (5), 1809−1825.
(32) De Poli, M.; Zawodny, W.; Quinonero, O.; Lorch, M.; Webb, S. J.; Clayden, J. Conformational Photoswitching of a Synthetic Peptide Foldamer Bound within a Phospholipid Bilayer. *Science* **2016**, *352* (6285), 575−580.
(33) Chudgar, R. J. Azo Dyes. *Kirk-Othmer Encyclopedia of Chemical Technology*, 5th ed.; Wiley, 2000; Vol. *9*.
(34) Frisch, M. J.; Trucks, G.; Schlegel, H.; Scuseria, G.; Robb, M.; Cheeseman, J.; Scalmani, G.; Barone, V.; Mennucci, B.; Petersson, G.; et al. *Gaussian 09*, Revision D.01; Gaussian Inc.: Wallingford, CT, 2009.
(35) Mewes, S. A.; Plasser, F.; Dreuw, A. Communication: Exciton Analysis in Time-Dependent Density Functional Theory: How Functionals Shape Excited-State Characters. *J. Chem. Phys.* **2015**, *143* (17), 171101.
(36) Laurent, A. D.; Jacquemin, D. TD-DFT Benchmarks: A Review. *Int. J. Quantum Chem.* **2013**, *113* (17), 2019−2039.
(37) Zheng, Q.; Chu, W.; Zhao, C.; Zhang, L.; Guo, H.; Wang, Y.; Jiang, X.; Zhao, J. Ab Initio Nonadiabatic Molecular Dynamics Investigations on the Excited Carriers in Condensed Matter Systems. *Wiley Interdiscip. Rev.: Comput. Mol. Sci.* **2019**, *9* (6), No. e1411.
(38) Tomasi, J.; Mennucci, B.; Cammi, R. Quantum Mechanical Continuum Solvation Models. *Chem. Rev.* **2005**, *105* (8), 2999−3094.
(39) Bandara, H. M.; Burdette, S. C. Photoisomerization in Different Classes of Azobenzene. *Chem. Soc. Rev.* **2012**, *41* (5), 1809−25.
(40) Guo, H.; Jing, Y.; Yuan, X.; Ji, S.; Zhao, J.; Li, X.; Kan, Y. Highly Selective Fluorescent Off-on Thiol Probes Based on Dyads of Bodipy and Potent Intramolecular Electron Sink 2,4-Dinitrobenzenesulfonyl Subunits. *Org. Biomol. Chem.* **2011**, *9* (10), 3844−53.
(41) Grabowski, Z. R.; Rotkiewicz, K.; Rettig, W. Structural Changes Accompanying Intramolecular Electron Transfer: Focus on Twisted Intramolecular Charge-Transfer States and Structures. *Chem. Rev.* **2003**, *103* (10), 3899−4032.
(42) Goulet-Hanssens, A.; Utecht, M.; Mutruc, D.; Titov, E.; Schwarz, J.; Grubert, L.; Bleger, D.; Saalfrank, P.; Hecht, S. Electrocatalytic Z–> E Isomerization of Azobenzenes. *J. Am. Chem. Soc.* **2017**, *139* (1), 335−341.
(43) Diau, E. W.-G. A New Trans-to-Cis Photoisomerization Mechanism of Azobenzene on the $S_1(n,\pi^*)$ Surface. *J. Phys. Chem. A* **2004**, *108* (6), 950−956.
(44) Tiago, M. L.; Ismail-Beigi, S.; Louie, S. G. Photoisomerization of Azobenzene from First-Principles Constrained Density-Functional Calculations. *J. Chem. Phys.* **2005**, *122* (9), 094311.

https://doi.org/10.1021/acs.jpca.1c00125
J. Phys. Chem. A 2021, 125, 3088−3094

(45) Cattaneo, P.; Persico, M. An Ab Initio Study of the Photochemistry of Azobenzene. *Phys. Chem. Chem. Phys.* **1999**, *1* (20), 4739−4743.
(46) Ma, H.; Peng, Q.; An, Z.; Huang, W.; Shuai, Z. Efficient and Long-Lived Room Temperature Organic Phosphorescence: Theoretical Descriptors for Molecular Designs. *J. Am. Chem. Soc.* **2019**, *141* (2), 1010−1015.
(47) Martin, R. L. Natural Transition Orbitals. *J. Chem. Phys.* **2003**, *118* (11), 4775−4777.

https://doi.org/10.1021/acs.jpca.1c00125
J. Phys. Chem. A 2021, 125, 3088−3094

Supporting Information

Modulating Charge Separation and Intersystem Crossing in Donor-Switch-Acceptor Systems : A Computational Study

Yuanyuan Chong[1], Xiaolong Zhang[1], Biao Chen[1], Ran Liu[1,3], Ziye Wu[1,4], Guoqing Zhang[1],

Jun Jiang[1], Shaul Mukamel[2]*, Guozhen Zhang[1]*

[1] *Hefei National Laboratory for Physical Sciences at the Microscale, CAS Center for Excellence in Nanoscience, School of Chemistry and Materials Science, University of Science and Technology of China, Hefei, Anhui 230026, P. R. China. E-mail: guozhen@ustc.edu.cn.*

[2] *Departments of Chemistry, and physics & astronomy, University of California, Irvine, CA 92697, USA. E-mail: smukamel@uci.edu.*

[3] *MOE Key Laboratory of Organic OptoElectronics and Molecular Engineering, Department of Chemistry, Tsinghua University, Beijing 100084, P. R. China.*

[4] *School of Information, Guizhou University of Finance and Economics, Guiyang 550025, P. R. China.*

Table of Contents

Computational method

All electronic structure calculations were performed using CAM-B3LYP functional as implemented in *Gaussian 09* program[1]. The calculation of SOC matrix elements was done with *PySOC* program[2] which connects MolSOC[3] and *Gaussian 09* software[1]. Multiwfn[4] (a multifunctional wavefunction analyzer) and VMD[5] (a molecular visualization program) were used for visualization of transition orbitals based on unrelaxed excited-state densities from time-dependent density functional theory (TDDFT)[6] calculations. Hefei-NAMD developed by Zhao et al. were used for examining the dynamics of excited electrons[7].

The ground state equilibrium structures of all molecules, including D-A systems and their derivative D-S-A systems molecules were optimized at the level of CAM-B3LYP/6-31G(d). TDDFT at the same level of theory were used for simulating electronic excited states of interest[6], from which we can get information on UV-vis absorption, excited state energy levels and photoexcited electron transition. The long-range corrected CAM-B3LYP functional[8] is known for better description of charge transfer excited states than conventional hybrid functionals like B3LYP and PBE0. The simulated luminescence properties of D-A system samples in agreement with experiment, validating the choice of CAM-B3LYP. Based on the optimized structures in excited states, we computed excitation energies at the level of CAM-B3LYP/6-311+G(d,p). The solvent effect of tetrahydrofuran was simulated using the polarizable continuum model (PCM)[9].

The ab initio time dependent non-adiabatic molecular dynamics (NAMD)

simulations are carried out using Hefei-NAMD code[7], which augments the Vienna ab initio simulation package (VASP)[10] with the NAMD capabilities within time domain Kohn Sham equation (TDKS)[11-12]. We performed the time-dependent ultrafast electron evolution process, assisted by the surface hopping algorithm of Hefei-NAMD. With a time step of 1 fs, a 1.0 ps microcanonical trajectory was generated under the tempecture of 300 K.

The fluorescence rate, $k_{FL} = \tau_{FL}^{-1}$, can be estimated as[13-14],

$$k_{FL} = \frac{e^2}{2\pi\varepsilon_0 m_e c^3 \hbar^2} \Delta E^2 f \quad (1)$$

Here, e is the electron charge; ε_0 is the vacuum permittivity; m_e is the electron mass; c is the speed of light; $\hbar$ is the reduced Planck constant; ΔE is the adiabatic energy difference between Sn and S0 states (i.e., E [S_0|S_n] $-$ E[S_n|S_n]) and f is the S_n-S_0 oscillator strength calculated at the S_n minimum.

Based on the Marcus theory, the qualitative ISC rate can be calculated using Eq. (2)[13, 15-17].

$$k_{ISC} = \frac{2\pi}{\hbar} |H_{SOC}|^2 \frac{1}{\sqrt{4\pi\lambda k_B T}} exp\left(-\frac{(\Delta G_{ST}^{v})^2}{4\lambda k_B T}\right) \quad (2)$$

Here, H_{SOC} is the SOC matrix element; λ is the reorganization energy (i.e., E [T_m|S_0] $-$ E[T_m|T_m]); ΔG_{ST}^{v} is the vertical Gibbs free energy gap between T_m and S_n (i.e., $\Delta G_{ST}^{v} \approx \Delta E_{ST}$, E[T_m|S_0] $-$ E[S_n| S_0]); k_B is the Boltzmann constant, and T is the absolute temperature 300 K. Then we can estimate the lifetime of ISC using the relation $k_{ISC} = \tau_{ISC}^{-1}$.

Absorption and emission of the D-A system

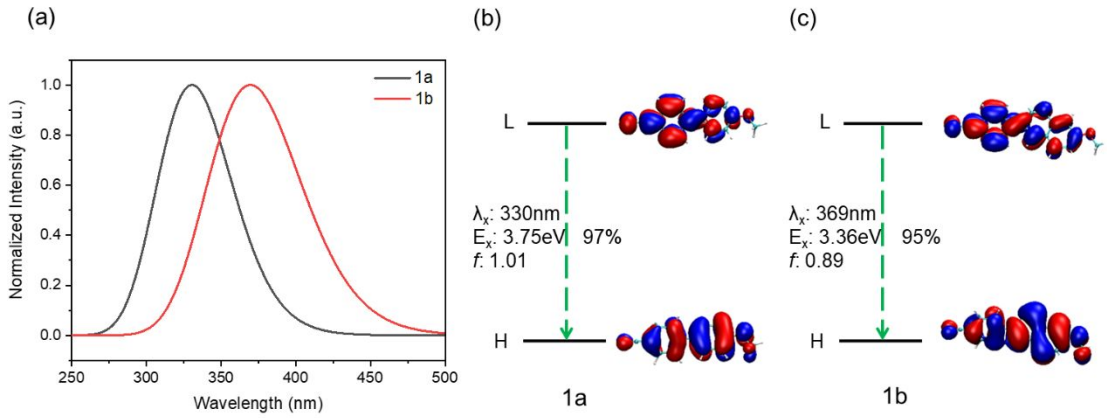

Figure S1. (a) The computed steady state emission spectrum of typical D-A molecules **1a** and **1b**. (b) and (c) Radiative electron transitions from the first excited state (S1) to the ground state (S0) in **1a** and **1b**, respectively. All calculations are based on cam-B3LYP functional with 6-31G(d) basis set in tetrahydrofuran solvent.

Table S1. Experimental and theoretical optical properties of typical D-A molecules **1a** and **1b** at room temperature in tetrahydrofuran solvent.

D-A	Absorbance			Luminescence		
	Experiment (nm)	Simulation (nm)	*f*	Experiment (nm)	Simulation (nm)	*f*
1a	296	271	0.95	352	330	1.01
1b	272	251	0.99	386	369	0.89

As shown in Figure S1 and Table S1, CAM-B3LYP give trends of fluorescent spectra for typical D-A system molecules, the following information can be described:

First, the absorption band and the emission peak of D-A system molecules simulated by CAM-B3LYP (absorption band: **1a** located in 271 nm, **1b** located in 251 nm; emission peak: **1a** located in 330 nm, **1b** located in 369 nm) approach to the experiment values (absorption band: **1a** located in 296 nm, **1b** located in 272 nm; emission peak: **1a** located in 352 nm, **1b** located in 386 nm) (Table S1).

Second, the radiative electron transitions from S_1 to S_0 is a local excited (LE) transition with a transition intensity (oscillation strength) close to 1. In the meantime, the donor and acceptor are conjugated in the same plane and iso-surface electron cloud density is distributed over the entire molecule (Figure S1b-c).

From the above, CAM-B3LYP can give a reasonable description of absorption and emission properties of D-A system molecules. Thus, we argue that CAM-B3LYP is a reasonable choice for DFT simulations about the subsequent D-S-A systems.

Electron transition of the trans- isomer D-S-A molecules in the excited state

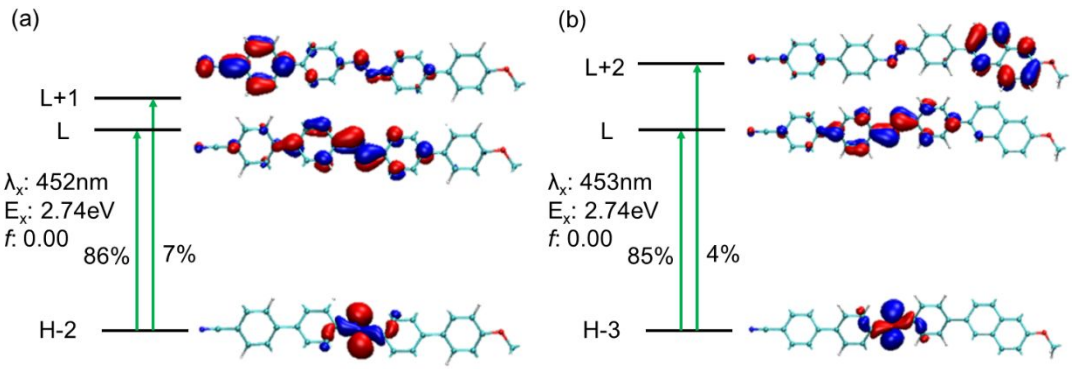

Figure S2. (a) and (b) Electron transition of the excitation to the first excited state (S_1) of trans-**1a** and trans-**1b**, respectively.

Table S2. The singlet excited state transition absorption information of D-S-A according to TDDFT calculation.

			Energy (eV)	Wavelength (nm)	Oscillator Strength (*f*)	Transition Configuration
1a	D-trans-A	S1	2.74	452	0	100 → 103 86%
		S2	3.50	354	1.98	102 → 103 78% 101 → 103 13%
		S3	4.92	276	0.07	101 → 103 73% 102 → 103 9%

	D-cis-A	S1	2.73	454	0.09	102 → 103 32% 101 → 103 25%
		S2	4.14	300	0.67	102 → 103 48% 95 → 103 11%
		S3	4.46	278	0.48	101 → 103 46% 100 → 103 31%
1b	D-trans-A	S1	2.74	453	0	112 → 116 85%
		S2	3.47	358	2.11	115 → 116 60% 114 → 116 29%
		S3	4.22	294	0.17	115 → 118 32% 114 → 116 30%
	D-cis-A	S1	2.73	454	0.10	114 → 116 42% 115 → 116 14%
		S2	4.02	308	0.70	115 → 116 49% 115 → 118 10%
		S3	4.29	289	0.11	115 → 118 50% 115 → 119 6%

In trans- D-S-A system molecules, the main electron transitions of S_1 contain an n-π* transition on the Azo moiety and a little charge transfer transition from switches to acceptors with a transition intensity *f*=0.00 (Figure S2). This means that the S_1 state is a "dark state" with forbidden transition and non-fluorescent emission[18].

Potential energy surface scanning along the rotation pathway

Table S3. Natural Bond Orbitals (NBO) charge profiles of the whole Azo part and the N=N moiety of trans-1a and trans-1b in their ground states and the second singlet excited states.

trans-1a	S_0	N=N	-0.39
		Azo	-0.01
	S_2	N=N	-0.59
		Azo	-0.11
trans-1b	S_0	N=N	-0.39
		Azo	-0.00
	S_2	N=N	-0.58
		Azo	-0.15

Table S3 shows that the N=N moiety of Azo and the whole Azo part as well gain electrons as trans-1a and trnas-1b are excited to their S_2 states.

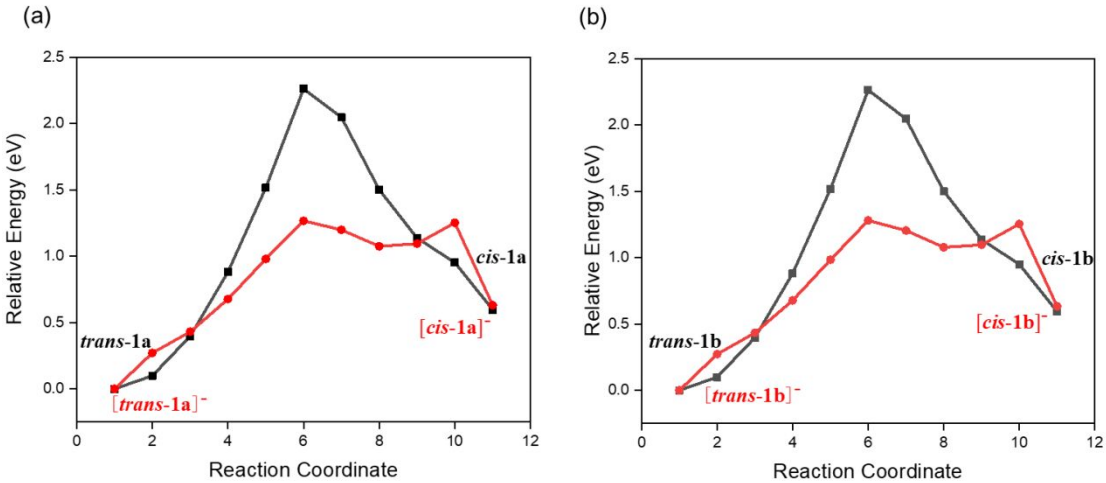

Figure S3. Potential energy surface scan of neutral and anion D-S-A along isomerized rotation pathway

Relaxed potential energy surface scan of neutral and anion D-S-A along isomerized rotation pathway, whose dihedral angles are 180°, 163°, 146°, 129°, 112°, 95°, 78°, 61°, 44°, 27°, 9.8°, respectively. Compared with neutral molecules, the anionic D-S-A has substantially lower isomerization energy barrier, meaning its isomerization will be accelerated.

The Ultrafast electron evolution

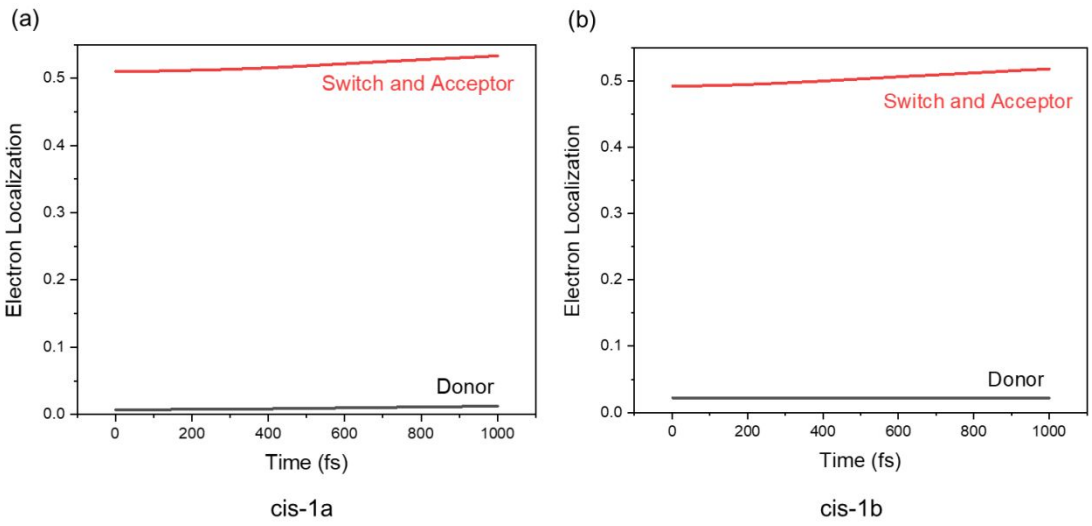

Figure S4. Time-dependent spatial electron distribution for electron at 300 K of cis-**1a** (a) and cis-**1b** (b).

As shown in Figure S4(a), in cis-**1a** configuration (charge transport channel is "OFF" state), electrons transferred to the part of switch and acceptor hardly transfer back within 1 ps. It is manifested that transferred electron and remained hole recombination hardly in the cis- form of D-S-A, which break the conjugated configuration.

Cis-**1b** (Figure S4b) has the same regular as cis-**1a**.

NTO of cis- isomer in the first triplet excited state

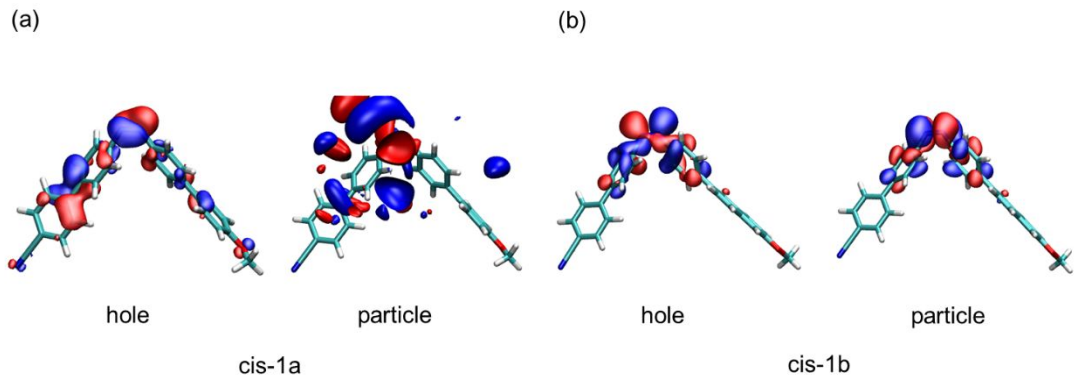

Figure S5. The dominant natural transition orbital pairs for T_1 state of cis-1a and cis-1b.

We calculated the dominant natural transition orbital (NTO)[19] pairs for T1 state of cis- forms to demonstrate that the electron trap exists in triplet states after ISC process. In figure S5, the iso-surface of frontier Kohn-Sham orbitals retains in the part of switch and acceptor both before and after transition. It indicates that the electrons transferred from donor stay at the part of switch and acceptor in the triplet state.

The extendibility of the established D-S-A model

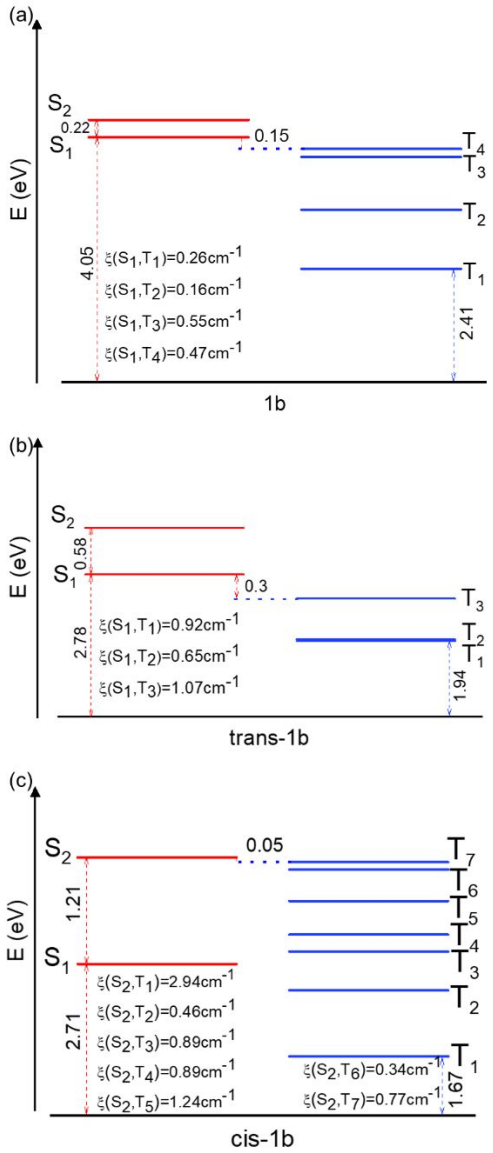

Figure S6. Energy level diagrams of excited states and SOC coefficients (ξ) between

different singlet-triplet ISC channels for **1b** (a), trans-**1b** (b) and cis-**1b** (c). Red lines represent singlet excited state energy levels and blue lines represent triplet excited state energy levels.

Table S4. S_1-S_0 (1b) or S_2-S_0 (trans-1b and cis-1b) energy gap ΔE and oscillator strength f at the S_1 minimum (**1b**) or S_2 minimum (trans-**1b** and cis-**1b**) structures. Fluorescence rate (k_{FL}) and fluorescence lifetime (τ_{FL}) of molecules **1b**, trans-**1b** and cis-**1b**.

	ΔE (eV)	f	k_{FL} (10^8 s^{-1})	τ_{FL} (ns)
1b（S_1）	-3.36	0.89	4.37	2.29
trans-1b（S_2）	-2.73	1.61	5.24	1.91
cis-1b（S_2）	-2.89	0.84	3.06	3.27

Table S5. Sn-Tm energy gap (ΔE_{ST}), reorganization energy (λ), and SOC coefficients (V_{SOC}) at the S_0 minimum structures. ISC rate (k_{ISC}), ISC rate relative to D-A system molecule 1b (k_{rel}) and ISC lifetime (τ_{ISC}) of molecules **1b**, trans-**1b** and cis-**1b**.

		ΔE_{ST}(eV)	λ(eV)	V_{SOC} (cm^{-1})	k_{ISC} (s^{-1})	k_{rel}	τ_{ISC} (s)
1b	S_1-T_4	-0.15	-0.21	0.47	4.55×10^7	1	2.20×10^{-8}
trans-1b	S_1-T_3	-0.30	-0.57	1.07	8.28×10^7	1.82	1.21×10^{-8}
cis-1b	S_1-T_2	-0.30	-0.10	0.95	1.20×10^5	$2.64*10^{-3}$	8.32×10^{-6}
	S_2-T_7	-0.05	-0.70	0.77	1.78×10^8	3.91	5.61×10^{-9}

The structure of **1b** donor contains a para-methoxy-naphthalene ring as shown in Figure 1a. Like cis-**1a**, the value of $\Delta E_{S_1S_2}$ (1.21 eV) in cis-**1b** is much larger than its $\Delta E_{S_2T_7}$ (0.05 eV). Consequently, the associated competing processes to ISC in cis-**1b**, including VR, IC and fluorescence emission, are all suppressed, thus such case is beneficial to the ISC process from S_2.[20] This is supported by the comparison of changes in fluorescent emission rates (**1b**: 4.37×10^8 s^{-1} → cis-**1b**: 3.06×10^8 s^{-1}) and ISC rates (**1b**: 4.55×10^7 s^{-1} → cis-**1b**: 1.78×10^8 s^{-1}) in Table S5. As Figure S6 and Table S5 present, the major ISC channels, their corresponding ΔE_{ST} values and SOC coefficients in **1b** family is similar to the counterpart properties in **1a** family, suggesting our proposed D-S-A model can be applied to different D-A molecular systems for the

enhancement of ISC.

References

1. Frisch, M. J.; Trucks, G.; Schlegel, H.; Scuseria, G.; Robb, M.; Cheeseman, J.; Scalmani, G.; Barone, V.; Mennucci, B.; Petersson, G. et al., Gaussian 09, Revision D. 01, Gaussian. *Inc.: Wallingford, CT* **2009**.
2. Gao, X.; Bai, S.; Fazzi, D.; Niehaus, T.; Barbatti, M.; Thiel, W., Evaluation of Spin-Orbit Couplings with Linear-Response Time-Dependent Density Functional Methods. *J Chem Theory Comput* **2017,** *13* (2), 515-524.
3. Chiodo, S. G.; Russo, N., One-Electron Spin-Orbit Contribution by Effective Nuclear Charges. *J. Comput. Chem.* **2009,** *30* (5), 832-839.
4. Lu, T.; Chen, F., Multiwfn: A Multifunctional Wavefunction Analyzer. *J. Comput. Chem.* **2012,** *33* (5), 580-592.
5. Humphrey, W.; Dalke, A.; Schulten, K., Vmd: Visual Molecular Dynamics. *Journal of molecular graphics* **1996,** *14* (1), 33-38.
6. Laurent, A. D.; Jacquemin, D., TD-DDFT Benchmarks: A Review. *Int. J. Quantum Chem* **2013,** *113* (17), 2019-2039.
7. Zheng, Q.; Chu, W.; Zhao, C.; Zhang, L.; Guo, H.; Wang, Y.; Jiang, X.; Zhao, J., Ab Initio Nonadiabatic Molecular Dynamics Investigations on the Excited Carriers in Condensed Matter Systems. *Wiley Interdisciplinary Reviews: Computational Molecular Science* **2019**, e1411.
8. Mewes, S. A.; Plasser, F.; Dreuw, A., Communication: Exciton Analysis in Time-Dependent Density Functional Theory: How Functionals Shape Excited-State Characters. *J Chem Phys* **2015,** *143* (17), 171101.
9. Tomasi, J.; Mennucci, B.; Cammi, R., Quantum Mechanical Continuum Solvation Models. *Chem. Rev.* **2005,** *105* (8), 2999-3094.
10. Kresse, G.; Furthmüller, J., Software Vasp, Vienna (1999). *Phys. Rev. B* **1996,** *54* (11), 169.
11. Akimov, A. V.; Prezhdo, O. V., The Pyxaid Program for Non-Adiabatic Molecular Dynamics in Condensed Matter Systems. *J. Chem. Theory. Comput.* **2013,** *9* (11), 4959-4972.
12. Akimov, A. V.; Prezhdo, O. V., Advanced Capabilities of the Pyxaid Program: Integration Schemes, Decoherence Effects, Multiexcitonic States, and Field-Matter Interaction. *J. Chem. Theory. Comput.* **2014,** *10* (2), 789-804.
13. Liu, R.; Gao, X.; Barbatti, M.; Jiang, J.; Zhang, G., Promoting Intersystem Crossing of a Fluorescent Molecule Via Single Functional Group Modification. *J Phys Chem Lett* **2019,** *10* (6), 1388-1393.
14. Hilborn, R. C., Einstein Coefficients, Cross Sections, F Values, Dipole Moments, and All That. *Am. J. Phys.* **1982,** *50* (11), 982-986.
15. Marcus, R., Nonadiabatic Processes Involving Quantum-Like and Classical-Like Coordinates with Applications to Nonadiabatic Electron Transfers. *J. Chem. Phys.* **1984,** *81* (10), 4494-4500.
16. Englman, R.; Jortner, J., The Energy Gap Law for Radiationless Transitions in Large Molecules.

Molecular Physics **1970,** *18* (2), 145-164.
17. Ou, Q.; Subotnik, J. E., Electronic Relaxation in Benzaldehyde Evaluated Via Td-Dft and Localized Diabatization: Intersystem Crossings, Conical Intersections, and Phosphorescence. *J. Phys. Chem. C* **2013,** *117* (39), 19839-19849.
18. Guo, H.; Jing, Y.; Yuan, X.; Ji, S.; Zhao, J.; Li, X.; Kan, Y., Highly Selective Fluorescent Off-on Thiol Probes Based on Dyads of Bodipy and Potent Intramolecular Electron Sink 2,4-Dinitrobenzenesulfonyl Subunits. *Org Biomol Chem* **2011,** *9* (10), 3844-53.
19. Martin, R. L., Natural Transition Orbitals. *J. Chem. Phys.* **2003,** *118* (11), 4775-4777.
20. Xu, Y.; Liang, X.; Zhou, X.; Yuan, P.; Zhou, J.; Wang, C.; Li, B.; Hu, D.; Qiao, X.; Jiang, X.; Liu, L.; Su, S. J.; Ma, D.; Ma, Y., Highly Efficient Blue Fluorescent Oleds Based on Upper Level Triplet-Singlet Intersystem Crossing. *Adv. Mater.* **2019**, e1807388.